LONG-TIME DRAINING OF THIN LIQUID FILMS IN BUCKLED LUNG AIRWAYS

J. Rosenzweig
Centre for Computational Science, Queen Mary & Westfield College,
Mile End Road, London E1 4NS, UK
J.Rosenzweig@qmw.ac.uk

O. E. Jensen
Division of Theoretical Mechanics, School of Mathematical Sciences,
University of Nottingham, University Park, Nottingham NG7 2RD, UK
Oliver.Jensen@nottingham.ac.uk

Abstract The peripheral airways of the lung are deformable and are lined with a thin layer of liquid. Here we examine how surface tension and bending stresses together determine the equilibrium configurations of an airway, which we model as an axially uniform, liquid-lined elastic tube. Conditions are identified under which capillary forces can induce collapse and flooding of the airway. We then describe the large-time asymptotics of unsteady liquid-lining flows within deformed airways and on other surfaces of prescribed nonuniform curvature.

Keywords: Capillary-elastic instabilities; surface-tension-driven flows.

1. INTRODUCTION

The lung is formed from a network of bifurcating, liquid-lined airways. Of the 23 generations of airways, those beyond generation 12 in an adult lung have diameters of 1mm or less. At these small lengthscales, surface tension can have a major influence on airway mechanics. In particular, subatmospheric capillary pressures in an airway's liquid lining impose a compressive stress on the deformable airway wall that may cause the wall to buckle and collapse. This is resisted by bending stresses in the wall. In Section 2 we explore this competition by modelling an airway as an axially uniform, liquid-lined, thin-walled elastic tube. We show how capillary-elastic interactions give rise to hysteresis in the quasi-static

inflation-deflation cycle, and we identify conditions under which surface tension can cause abrupt airway flooding and collapse.

Since the distribution of the liquid lining is crucial in controlling the shape and stability of small buckled airways, it is important to understand the dynamics of draining flows following abrupt changes in airway geometry. In Section 3 we consider surface-tension-driven flows of thin liquid films coating substrates of fixed shape (mimicking a buckled airway wall) but having nonuniform curvature. By solving the governing lubrication equations numerically, and asymptotically at large times, we show how the liquid typically drains to form puddles or drops of uniform pressure, joined by narrow regions where the film is very thin. For flows in bounded spatial domains, we find that these narrow regions may be described by up to three consecutive self-similar asymptotic solutions. Two of these, for which the minimum film thickness $h_{\min}$ has algebraic time-dependence, are well known (Jones and Wilson 1978; Hammond 1983; Wilson and Jones 1983; Jensen 1997). Prior to these, a new regime may arise for which $h_{\min}$ has logarithmic time-dependence, and for which film shapes resemble that near an advancing contact line (Hocking, 1981). Finally, we show in Section 4 that for flows in unbounded domains (draining off a localised hump, or in an interior corner), further novel self-similar structures arise with intricate time-dependence.

2. CAPILLARY-ELASTIC INSTABILITIES

We consider an axially uniform, thin-walled elastic tube coated internally with a liquid layer of uniform capillary pressure, and loaded externally by a uniform pressure pD/R^3 (where D is the bending stiffness of the tube wall and R is the tube's undeformed radius). The internal air pressure is taken to be zero. Various post-buckled equilibrium configurations of the tube are illustrated in Figure 1. The tube's shape is governed by Euler–Bernoulli beam theory, so that its curvature κ/R satisfies, as a function of arc-length Rs (Tadjbakhsh & Odeh, 1967),

$$\kappa_{ss} + \tfrac{1}{2}\kappa^3 - c\kappa = \mathcal{P}. \tag{2.1}$$

Here $\mathcal{P}(s)$ is the dimensionless negative transmural pressure, and c is a constant of integration. Where the wall is wet, $\mathcal{P} = p + \sigma/a$, where aR is the radius of curvature of the nearest air-liquid interface and $\sigma = \sigma^* R^2/D$ is a dimensionless parameter relating surface tension σ^* to bending forces. Where the wall is effectively dry, $\mathcal{P} = p + \sigma\kappa$, a condition which is derived from a force balance at each contact line (Hill, Wilson & Lambert 1997), where the meniscus wets the wall with zero contact angle. Equation (2.1) is solved subject to boundary conditions

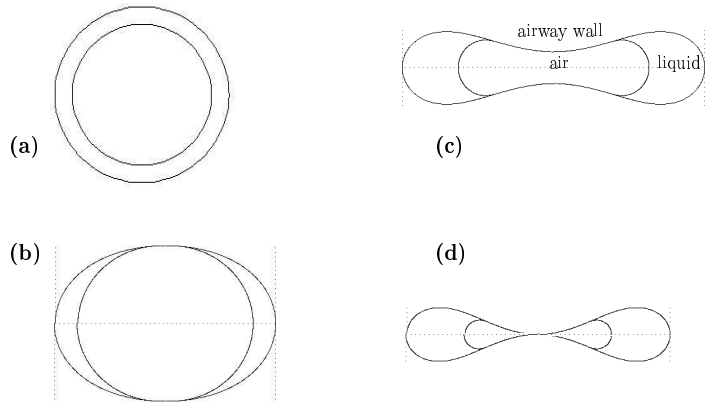

Figure 1 The tube is initially circular and lined with a film of uniform thickness (a). As p is increased, the tube buckles (in this example into two lobes), and the film ruptures (b,c,d) to form a capillary meniscus, leaving a part of the wall effectively dry. Opposite wall contact is illustrated in (d).

of membrane inextensibility, fixed liquid volume per unit length of tube $V_l R^2$ and symmetry, assuming buckling occurs in n lobes where $n \geq 2$. For full details of the model and its asymptotic and numerical treatment see Rosenzweig (2000) and Rosenzweig & Jensen (2001).

The model is parametrised by the external pressure p, the dimensionless surface tension σ, the liquid volume $V_l\,(< \pi)$ and the wavenumber n. Tethering to surrounding tissue, and the composite and heterogeneous structure of the airway wall, may cause the airway to buckle with $n > 2$ (Hill *et al.* 1997). Figure 2 shows results for the simpler two-lobed collapse of the tube (as in Figure 1) in the form of $p - V$ diagrams, where V is the total volume (per unit length) enclosed within the tube. Figure 2(a) shows $p - V$ curves for $V_l = 0.2\pi$. As σ is increased (e.g. to $\sigma = 0.6$), a fold appears in the $p - V$ curve, implying hysteresis in the quasi-steady inflation-deflation cycle. The post-buckled collapsed states are re-stabilised by opposite wall contact; solution branches extend until V is close to V_l. Although not resolved in the figure, as the meniscus approaches the point of wall contact, its curvature rises rapidly, the liquid pressure falls and the curve folds back rapidly as the tube floods, with $p \propto -\sigma(V - V_l)^{-2/3}$ as $V \to V_l$. Figure 2(b) shows analogous curves for $V_l > V_{crit}$, where $V_{crit} = 0.2694\pi$ is the total volume at the first point of opposite wall contact (Figure 1d). In this case the tube always floods before opposite wall contact can occur; solution curves have $p \sim -\sigma\sqrt{\pi}\,(V - V_l)^{-1/2}$ as $V \to V_l$. A weakly nonlinear analysis of the primary buckling bifurcation of the circular state (with $V = \pi$) shows

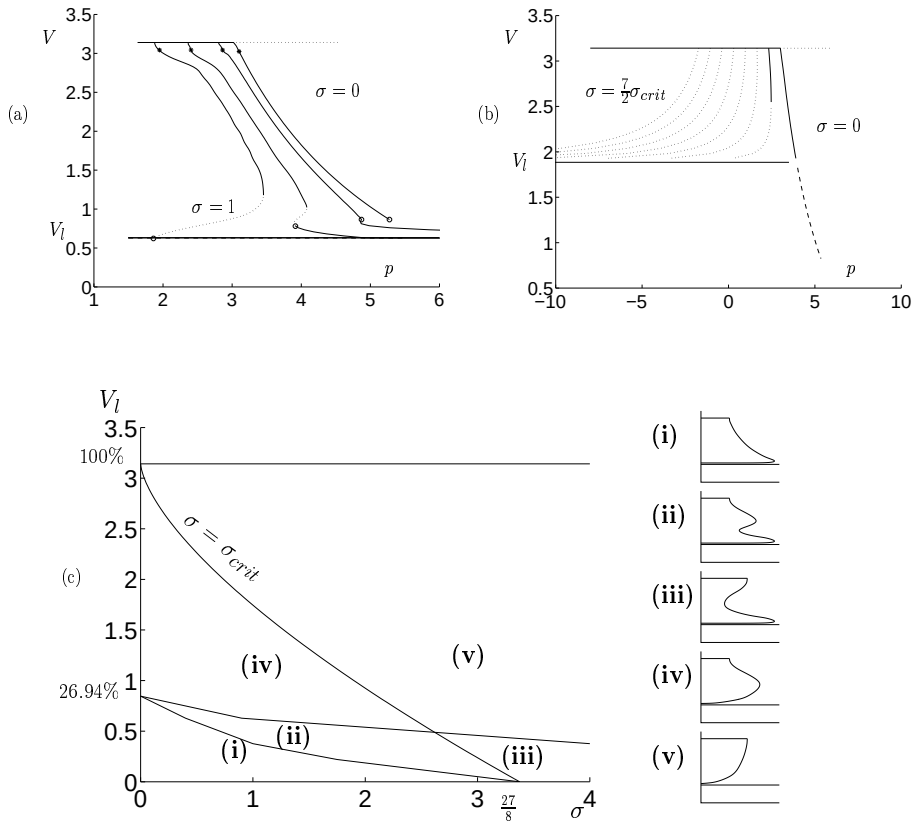

Figure 2 Results for two-lobed buckling. $p - V$ curves are shown for (a) $V_l = 0.2\pi$; $\sigma = 0, 0.2, 0.6, 1$, with rupture of the air-liquid interface denoted by * and opposite wall contact by o; and (b) $V_l = 0.6\pi$; $\sigma = 0, 0.5, 1, ... \times \sigma_{crit}$. Solid (dashed) lines show stable (unstable) solutions when p is the control parameter. (c) shows (σ, V_l)-parameter space, summarising possible shapes of the $p - V$ curve for $\sigma > 0$.

that for any $V_l < \pi$, the bifurcation is supercritical for $\sigma < \sigma_{crit}$, where

$$\sigma_{crit} = \frac{3}{2}\frac{(n^2-1)^2}{n^2}\left(1 - \frac{V_l}{\pi}\right)^{3/2},$$

and is subcritical otherwise. Thus for sufficiently large σ and V_l (as in Figure 2b), as p is increased the initially circular tube will always collapse abruptly to a completely flooded state. This represents an important mechanism of airway occlusion, which is irreversible in the present model, analogous to the 'compliant collapse' of axially uniform, axisymmetric airways identified by Halpern & Grotberg (1992).

A global picture of the (σ, V_l) parameter space for $n = 2$ is shown in Figure 2(c). Regions (i)–(v) correspond to the five distinct types of

(p, V)-curve that can arise. $\sigma = \sigma_{crit}$ provides one boundary; the other boundaries correspond to the appearance or disappearance of folds in the (p, V) curve. For low but positive σ and low V, $p - V$ curves are monotonic until the tube is close to flooding (region (i)). Increasing σ (modelling a surfactant-deficient or emphysematous lung), even at very low liquid volumes, introduces hysteresis in the inflation-deflation cycle that can lead to abrupt airway collapse (e.g. region (iii)). Similar behaviour was found by Heil (1999) in a 3D calculation. Increasing V (as might occur in pulmonary oedema) always leads to abrupt airway flooding from relatively large tube volumes, even at very low σ. Broadly similar results have also been obtained for buckling to modes with $n > 2$ (see also Hill *et al.* 1997).

3. THIN FILM FLOWS

Since the configuration of the liquid lining plays such an important role in determining the stability of a small airway, it is of obvious interest to examine flows of the liquid arising from abrupt changes in airway geometry. To concentrate purely on the fluid-mechanical aspects of this problem, we consider the draining of a liquid film of initially uniform thickness coating a substrate with fixed, non-uniform curvature. For thin films and weak curvature gradients, lubrication theory implies that at leading order the film thickness $h(x, t)$ satisfies, in suitable dimensionless variables (Schwartz & Weidner 1995),

$$h_t + \left(h^3(h_{xx} + \kappa)_x\right)_x = 0, \tag{3.1}$$

where t is time, x arclength along the substrate, and $\kappa(x)$ substrate curvature. Flows are driven by capillary pressure gradients dictated by the curvature $\kappa + h_{xx}$ of the film's free surface. Here we present some examples of 'typical' flows for two types of substrate geometry which we believe illustrate important general properties of this class of flows.

3.1. BOUNDED GEOMETRIES

As a first example, we consider a sinusoidal substrate with a profile $y = \cos x$, for which $\kappa = -\cos x$, and assume initially $h(x, 0) = \bar{h} < 1$. This models the readjustment of an initially uniform liquid film lining one lobe of a buckled airway. The evolution of the free surface and fluid pressure $p = -\kappa - h_{xx}$, under periodic boundary conditions, are shown in Figure 3(a,b). The film drains from the peaks of the substrate into the trough, until most of the film is concentrated in a large puddle at the trough, with small droplets remaining trapped at the peaks. For $t \gg 1$ the pressure in the puddle is at leading order uniform and negative, and

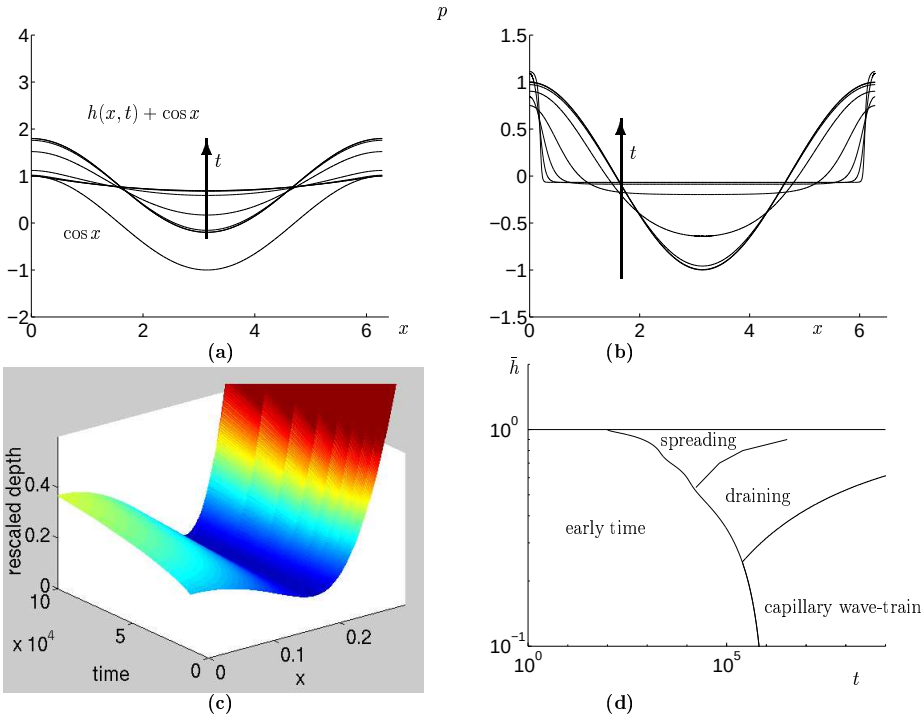

Figure 3 Draining from a sinusoidal substrate. The evolution of (a) film thickness and (b) fluid pressure is shown for $10^{-3} \leq t \leq 1.5 \times 10^4$, with $\bar{h} = 0.8$. (c) shows a blow-up of the asymptotic draining region, with h scaled on its minimum value. (d) shows a sketch of $(\bar{h}, t)$ parameter space.

in the droplets it is also uniform but positive; each droplet is connected to a puddle by an asymptotically narrow inner region (blown up in Figure 3c) across which the pressure changes by $\mathcal{O}(1)$ (Figure 3b).

Labelling the location of the left-hand inner region $x_p(t)$ and integrating (3.1) once over the droplet, the quasi-steady film thickness near $x = x_p$ satisfies

$$h^3 h_{xxx} = \dot{x_p} h - \dot{V} + h^3 \kappa_x(x_p), \tag{3.2}$$

where $V(t)$ is the volume of the droplet in $0 \leq x < x_p$. Using a combination of singular perturbation theory and numerical solution of (3.1), we found three consecutive late-time asymptotic draining regimes involving different balances of terms in (3.2).

- After an initial transient phase, and for sufficiently large $\bar{h}$, the flow is governed by the dominant balance $h^3 h_{xxx} \sim \dot{x_p} h$, resulting in the motion of the local film minimum given by the scaling

$$x_p \propto (t/\ln t)^{1/7},$$

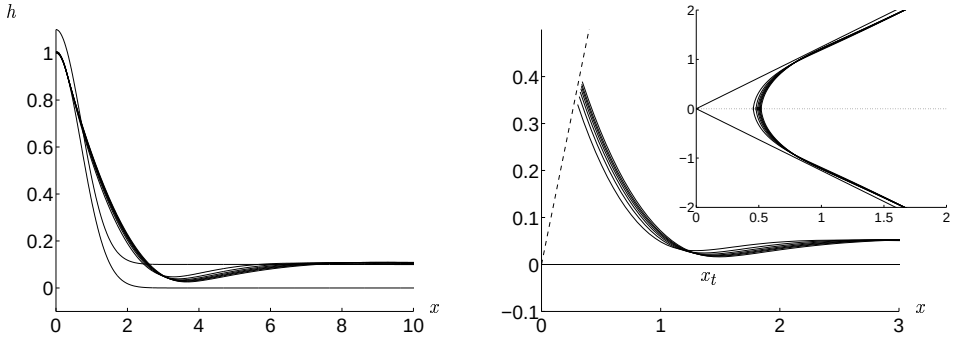

Figure 4 Draining (a) from a localised hump (of shape e^{-x^2}, $0 < t \leq 10^4$, $\bar{h} = 0.1$) and (b) into an interior corner (of internal angle $4\pi/7$, $0 < t \leq 10^3$).

with $h_{\min} \propto t^{-4/7}(\ln t)^{-2/21}$. This regime we call 'spreading,' since the same balance of terms arises in models of droplets advancing on solid surfaces (Hocking, 1981).

- Then, the film minimum stops sliding and the dominant balance changes to $h^3 h_{xxx} \sim -\dot{V}$, giving the flow rate out of the droplet as $-\dot{V} \propto t^{-5/4}$, with $h_{\min} \propto t^{-1/4}$; this regime we call 'draining'.
- Finally, at late times the forcing term comes in at leading order and generates the late time balance $h^3 h_{xxx} \sim -\dot{V} \sim h^3 \kappa_x \gg \dot{x_p} h$, which creates a capillary wave train on the droplet, with the flow rate $-\dot{V} \propto t^{-3/2}$; this regime we call 'capillary wave-train'.

The second and third regimes have been described in a number of previous studies (Jones & Wilson, 1978; Hammond 1983; Wilson & Jones, 1983), including one concerned with draining on non-uniformly curved substrates (Jensen, 1997). The first regime has not previously been identified in this context. Approximate asymptotic boundaries showing when each of these regimes is dominant are shown in Figure 3(d).

A critical feature of the geometry for this draining flow is that the puddle collecting the fluid is stationary, so that its pressure is independent of time. In unbounded domains this is not the case, and the resulting flows are significantly different.

3.2. UNBOUNDED GEOMETRIES

Two examples of draining on unbounded substrates are illustrated in Figure 4. The geometries correspond to (a) a localised hump and (b) an interior corner (solved by replacing h_{xx} in 3.1 with an expression for the

full curvature). In both cases a puddle forms (at the base of the hump, or filling the corner); the pressure in the puddle is lower than that of the film in the far field, so the puddle grows quasi-steadily and indefinitely by drawing in fluid from the far field. The rate at which the puddle grows is restricted by the diminishing film depth at its leading edge at $x = x_t(t)$; in both cases the local film minimum advances slowly while the film continues to thin. A spatially damped capillary wave propagates outwards from this minimum into the far field. At the same time small droplets are trapped on the top of the hump, as described in Section 3.

The late-time asymptotic structures of both flows in Figure 4 are similar, but they are significantly more complicated than in the bounded case. In the far field the capillary wave with amplitude $h-\bar{h} = \mathcal{O}(\epsilon(t)) \ll 1$ propagates outwards a distance $\mathcal{O}(t^{1/4})$. Rosenzweig (2000) gives scaling arguments and asymptotics for the regions connecting the linearised wave to the minimum at $x = x_t$ (which is of the 'draining' type). For the corner problem, these arguments suggest that $x_t \propto (\ln t)^{2/3}$ and $\epsilon \propto t^{1/20}(\ln t)^{-1/15}$; the hump problem is degenerate, and scaling suggests that $x_t \propto t^{\delta}$ and $\epsilon \propto t^{(1-4\delta)/20}$ for some eigenvalue δ. These predictions are consistent with numerical results, which suggest that $\delta \approx 0.0506$. Whether or not $\delta = 1/20$ remains to be established; unfortunately categorical numerical confirmation of these delicate scalings was not possible, partly because in both cases ϵ grows with time, so that these scalings only apply over long but bounded time intervals.

Acknowledgements. JR was supported by an Elmore Studentship, awarded by Gonville & Caius College, University of Cambridge.

References

Halpern, D., & Grotberg, J.B. (1992) *J. Fluid Mech.* **244**, 615–632.
Hammond, P. S. (1983) *J. Fluid Mech.* **137**, 363–384.
Heil, M. (1999) *J. Fluid Mech.* **380**, 309–337.
Hill, M. J., Wilson, T. A. & Lambert, R. K. (1997) *J. Appl. Physiol.* **82**, 233–239.
Hocking, L. M. (1981) *Q. J. Mech. Appl. Math.* **34**, 37–55.
Jensen, O.E. (1997) *J. Fluid Mech.* **331**, 373–403.
Jones, A.F. & Wilson, S. D. R. (1978) *J. Fluid Mech.* **87**, 263–288.
Rosenzweig, J. (2000) *Ph.D. Thesis*, University of Cambridge.
Rosenzweig, J. & Jensen, O. E. (2001), *submitted for publication.*
Schwartz, L. W. & Weidner, D. E. (1995) *J. Engng. Math.* **29**, 91–103.
Tadjbakhsh, I. & Odeh, F. (1967) *J. Math. Anal. Appl.* **18**, 59–74.
Wilson, S. D. R. & Jones, A. F. (1983) *J. Fluid Mech.* **128**, 219–230.